The International Journal of Engineering and Science (IJES)
|| Volume || 10 || Issue || 3 || Series II || Pages || PP 33-43|| 2021 ||
ISSN (e): 2319-1813 ISSN (p): 20-24-1805

CFD Analysis of Supersonic C-D Nozzle for Optimization of Divergent Angle

Goyal S.[1], Singh S.[2]
[1]*Automobile Design Engineer, Aftersales Department, Bentley Motors, Crewe, England, United Kingdom*
[2]*Senior Engineer, Plant Integrity Department, L & T Chiyoda Ltd, Vadodara, India*

ABSTRACT
The convergent-divergent nozzles with varying cross-sections are designed and are investigated by numerical simulations. Variation in divergent angle is made from 4.76° to 10° keeping all input parameters constant. Velocity, pressure, and Mach number contours are computed for every nozzle configuration obtained. Results report the direct proportion of velocity obtained at the outlet with the divergent angle when the computation is done considering the turbulence model. The results at the optimized divergent angle are calculated by analytical formulation in parallel and the mathematical results are found in good conformation with the analytical solution. Results so obtained show that even the slight variation of 0.01° in divergent angle above the optimized value shows reverse flow. An increment from 3% to 9 % in outlet velocity is found for an increase in the divergent angle which significantly affects the thrust generated at the nozzle outlet. Also, a significant increment from 13% to 20% is found in Mach number. This thrust can be consumed as a source of energy or power for taking off airplanes with a short runway which will also propose an innovation of rotor for airplanes instead of wings.
KEYWORDS:-*ICEM, C-D nozzle, Mach number, Divergent angle, Reverse flow*

Date of Submission: 12-03-2021 Date of Acceptance: 27-03-2021

I. INTRODUCTION

CD nozzle analysis is one of the standard CFD models of compressible fluid flow. The prime impact of compressibility of the fluid flow is displayed by shocks occurring within the flow whose accurate prediction is defiance to the CFD, to tackle this it is employed with special numerical schemes along with the fine grid [1]. The aim of the current work is achieved by varying the nozzle divergent angle from 4.76° to 10°. Here CFD proves its reliability by giving the results very close to the actual process and there is very little deviation in computational and analytical results.

The nozzle has gained huge importance due to its applications in propulsion systems. Employment of better performance nozzle in propulsion systems can be a sound way of coping up with the challenges in propulsion. Thus many researchers [2], [3] have carried out their work in proposing an efficient nozzle design. K. P. S. Surya Narayana et al. [4] determined the pressure, Mach number, cell Reynolds number, etc. for different mesh qualities. D. D. Majil [5] applied the Taguchi DOE method of optimization in determining the optimum nozzle parameters for various thrust vectoring configurations. K. M. Pandey et al. [6] observed the pressure contours, temperature contours, and turbulence intensity contours and Mach numbers for nozzle divergent angle 7.12°, 4°, 8°, 12°, and 16°. B. Kuttan P. et al. [7] found the optimum divergent angle for rocket nozzle by analyzing the Mach number, pressure, and turbulent intensity at the outlet for different geometries. G. Satyanarayana et al. [8] studied the nozzles of the various cross-sectional area and found that the rectangular cross-sectional area gives maximum outlet velocity. G. R. Rao et al. [9] analyzed C-D nozzle and found that mass flow rate decrease monotonically with Mach numbers and also variation in static pressure increases with Mach number less than 6. Shock wave formation occurs in a nozzle when the divergence angle is increased above a certain optimized valve. Shock waves recklessly harness the performance of the nozzle. K. G. Vishnu et al. [10] varied the divergence angle and studied the variation of shock structure with it. J. Wu et al. [11] also investigated supersonic bevelled nozzle jets to get a step ahead towards shock-free convergent-divergent jet nozzle.

II. THERORETICAL BACKGROUND

The convergent-divergent nozzle is analyzed and formulated to work at supersonic speeds. The flow-through nozzle is governed by the area-velocity relation.

$$\frac{dA}{dV} = \left(-\frac{A}{V}\right)(1 - \mathrm{M}^2) \qquad (1)$$

Mach number is a dimensionless quantity representing the ratio of flow velocity past a boundary to the local speed of sound.

$$M = \frac{V}{C} \qquad (2)$$

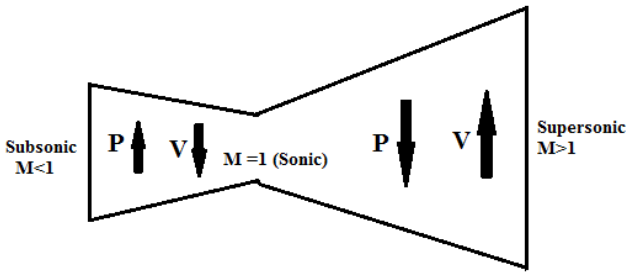

Figure 1: Flow Parameters In The C-D Nozzle

From the area-velocity relation and the above figure of the C-D nozzle, the following information can be deduced:

Table1:Basic Information Of Nozzle Parameters

M < 1, $\left(\frac{dA}{A}\right) < 0$	A decrease in area results in an increase in velocity and vice versa.
M = 1, $\left(\frac{dA}{A}\right) = 0$	Implies that where Mach number is unity, the area of the passage is either minimum or maximum.
M > 1, $\left(\frac{dA}{A}\right) > 0$	An increase in the area results in increases in velocity and vice versa.

III. ANALYTICAL METHODOLOGY

For the calculation of various parameters of nozzle i.e. pressure, temperature, density, velocity, Mach number, etc. can be calculated analytically. This analytical formulation is derived with the help of the basic governing equations according to which a compressible flow regulates. The basic equations for the calculation of the nozzle are as follows:

$$\frac{T_1}{T_2} = 1 + \left(\frac{\Upsilon-1}{2}\right) M^2 \frac{p_1}{p_2} = \left(\frac{T_1}{T_2}\right)^{\frac{\Upsilon}{\Upsilon-1}} = \left(1 + \left(\left(\frac{\Upsilon-1}{2}\right) M^2\right)\right)^{\frac{\Upsilon}{\Upsilon-1}} \qquad (3)$$

$$\frac{\rho_1}{\rho_2} = \left(\frac{T_1}{T_2}\right)^{\frac{1}{\Upsilon-1}} = \left(1 + \left(\left(\frac{\Upsilon-1}{2}\right) M^2\right)\right)^{\frac{\Upsilon}{\Upsilon-1}} \qquad (4)$$

$$\frac{A_2}{A^*} = \frac{1}{M}\left(\frac{2}{\Upsilon+1} + \left(\frac{\Upsilon-1}{\Upsilon+1}\right) M^2\right)^{\frac{\Upsilon+1}{2(\Upsilon-1)}} \qquad (5)$$

$$\frac{\dot{m}}{A_2} = \frac{p^*}{\sqrt{T^*}} \sqrt{\frac{\Upsilon}{R}} \frac{A^*}{A_2} \qquad (6)$$

IV. VALIDATION

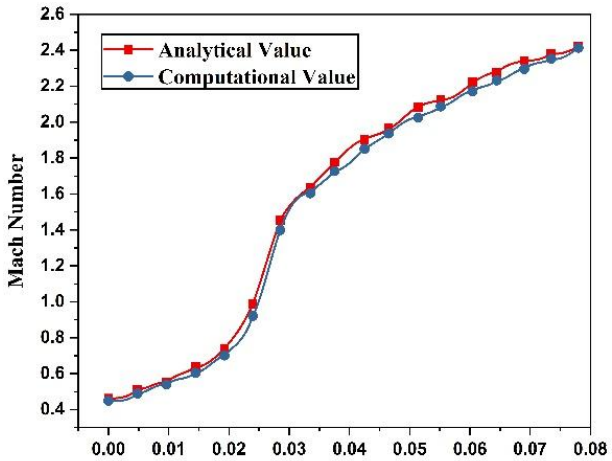

Figure 2: Analytical V/S Computational Values Of Mach Number In The C-D Nozzle

The computational result at the exit section of the nozzle of Mach number thus calculated is 2.4134 and that calculated analytically is 2.4190 at the optimized divergent nozzle angle of 9.5° and both the results are in good accordance with each other with an error of 0.2315 %.

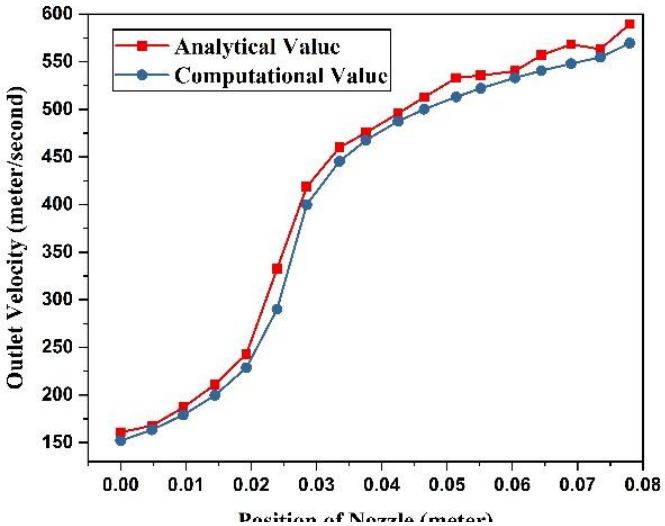

Figure 3: Analytical V/S Computational Values Of Outlet Velocity In The C-D Nozzle

The computational results of outlet velocity thus calculated is 569.5354 m/sec and that calculated analytically is 589.6013 m/sec at the optimized divergent nozzle angle of 9.5° and both the results are in good accordance with each other with an error of 3.4033 %.

V. COMPUTATIONAL METHODOLOGY AND IMPLEMENTATION

Governing Equations

The state of a flowing liquid is described by three variables namely the velocity, pressure p, and temperature T, and the governing equations are those of mass, momentum, and energy. Analysis of compressible flow of gases involves consideration of an additional variable, the fluid density ρ which is related to pressure and temperature by the characteristic gas equation:

$$pV' = mRT \text{ Or } pv' = RT \text{ Or } \frac{p}{\rho} = RT \qquad (7)$$

A dimensional analysis of the state equation would reveal that the gas constant R, though constant for a particular gas, is not dimensionless but has units of Joule/kg-K. For compressible analysis density-based solver is selected. The standard k-epsilon turbulence model is used for flow calculations as this models is found suitable by many researchers [6], [7], [8], [9]. The equations which govern a compressible flow through a nozzle are as follows:

Table2:Governing Equations Used For Flow Simulation

Continuity Equation	$\frac{d\rho}{\rho} + \frac{dA}{A} + \frac{dv}{v} = 0$(8)
Equation of State	$\frac{dp}{p} - \frac{d\rho}{\rho} - \frac{dT}{T} = 0$(9)
Momentum Equation	$\frac{dp}{\rho} + vdv = 0$(10)
Energy Equation	$dh + vdv = 0$ (11)
κ-ε Equation	$\frac{\partial \rho \kappa}{\partial t} + div(\rho u \kappa) = div\left[\left(\mu_t + \frac{\rho \mu_t}{\sigma_\kappa}\right) grad\kappa\right] + \rho\mu_t G - \rho\varepsilon$ (12) $\frac{\partial \rho \varepsilon}{\partial t} + div(\rho u \varepsilon) = div\left[\left(\mu_t + \frac{\rho \mu_t}{\sigma_\varepsilon}\right) grad\varepsilon\right] + C_{1\varepsilon}\rho\mu_t\left(\frac{\varepsilon}{\kappa}\right) - C_{2\varepsilon}\rho\frac{\varepsilon^2}{\kappa}$ (13)

Modelling of Nozzle

The Nozzle shapes are designed on ICEM as it is discussed above that the analysis is done for the different divergent angles of the nozzle. The lengths of the convergent and divergent parts are kept constant for each. This analysis is done for a range of divergent angle from 4.76° to 10°. The dimensions in millimeter (mm) of one of the nozzle are given as below:

Table3:Dimensional Information Of Nozzle

Inlet Width	15 mm
Throat Width	11 mm
Outlet Width	20 mm
Convergent Length	23.96 mm
Divergent Length	54.04 mm
Divergent Angle	4.76º

Blocking and meshing in ICEM

The 2-D planar mesh is created using the vertex and edge association method in ICEM. The mesh is refined near the walls and throat by certain mesh laws. The information regarding the mesh quality of the optimized nozzle are as follows:

Table4:Mesh Quality Report

Minimum Orthogonal Quality	9.86285e-01
Maximum Aspect Ratio	1.35064e+02
Nodes	61125
Quads	60512

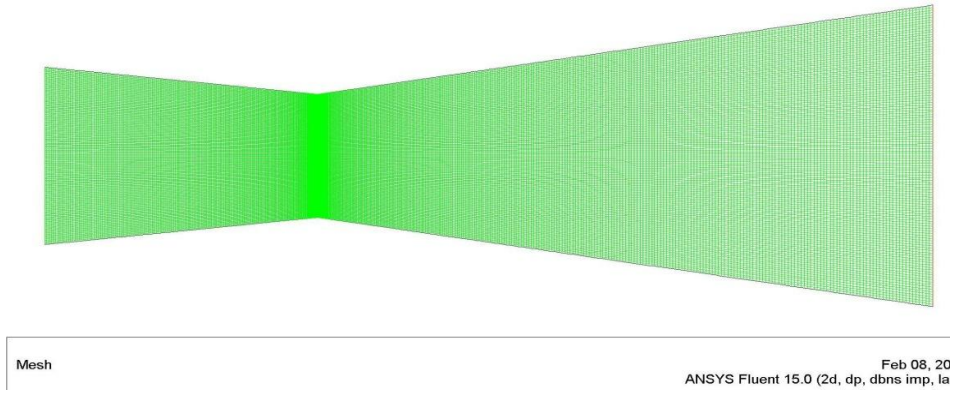

Figure 4: Mesh grid of the optimized nozzle

Solution Setup

Air, an ideal gas of temperature 300 kelvin is selected as fluid flowing in the nozzle. The inlet pressure condition is kept at 3 bar and outlet pressure is 0 bar. The analysis is done at Courant number 5 and Convergence criteria for continuity, velocity, and energy are taken to be 10^{-5}.

VI. RESULTS AND DISCUSSION

A very important and time-saving study is performed to carry out further investigation in the right direction. The grid-independent analysis is done to analyze the correct mesh size for simulation.

Table5:Results Of The Grid Independent Study

Case	No. of Elements	Maximum Outlet Velocity (m/sec)	Maximum Mach number
Case I	25802	583.5407	2.5459
Case II	36362	584.0735	2.5508
Case III	49882	584.0709	2.5516
Case IV	58427	584.0747	2.5512

Since variation in output parameters from case II to case III is negligible and a huge difference in the number of elements is there in both cases. The higher the number of elements higher will be the computational time and cost. So, case II is considered for further studies at different nozzle angles.

Divergent Angle 4.76°

Static pressure is a measurement of pressure when fluid is still or at rest. This analysis is a steady-state analysis so here we are talking about static pressure. It is very clear from the above contour that air expands in the nozzle because at the exit section pressure is getting down as compared to the inlet section. At the inlet, the pressure is observed in the range of 2.35e+05 Pascal to 2.55e+05 Pascal after then as the air moves towards to throat and the pressure near the throat of the C-D nozzle is observed in between 1.13e+05 Pa to 1.65e+05 Pa. After passing from the throat the fluid gets expand in the divergent section of the nozzle where the pressure gets low up to the exit section. From throat to exit section pressure varies from 1.13e+05 Pa to -5.97e+04 Pa.

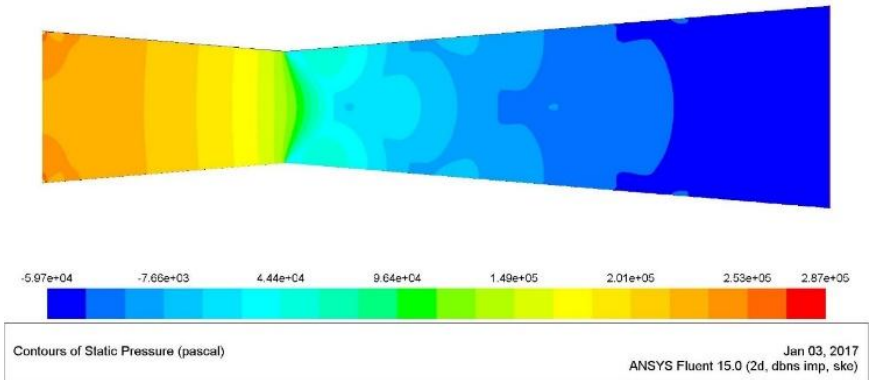

Figure 5: StaticPressure Contour at 4.76° Nozzle Angle

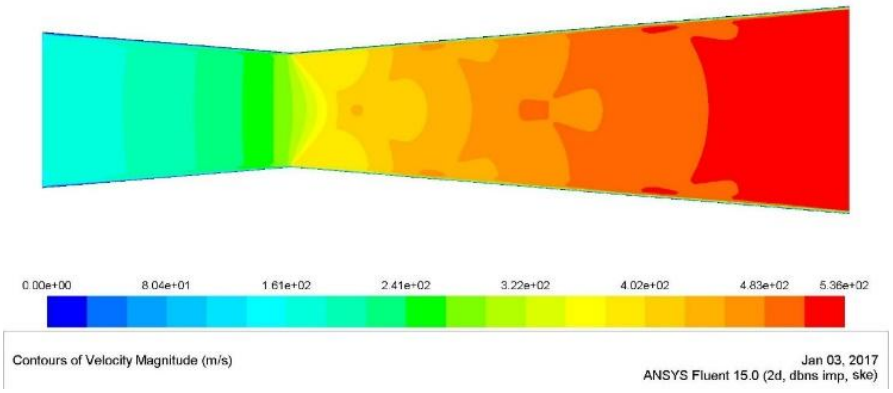

Figure 6: Velocity Contour at 4.76° Nozzle Angle

By the contour of velocity in fig. 6, it is clear that the flow is axis-symmetric. Through the graph of Mach number, it can be understand that just after the throat, Mach number is increasing it means there will be an increase in velocity also. At the entrance region of a nozzle, velocity is in between 160.85 m/sec to 187.55 m/sec. When fluid moves further the velocity measured just before the throat is around 200 m/sec and just after the throat there is a rise of one hundred in the velocity of flow. When fluid moves further in the divergent section there is a sudden increment in velocity and it becomes 428 m/sec from 300 m/sec and correspondingly Mach number varies from 1 to 1.7. As it is known that Mach number is directly proportional to the velocity of flow, so there will be the same pattern of rising in Mach number and velocity.

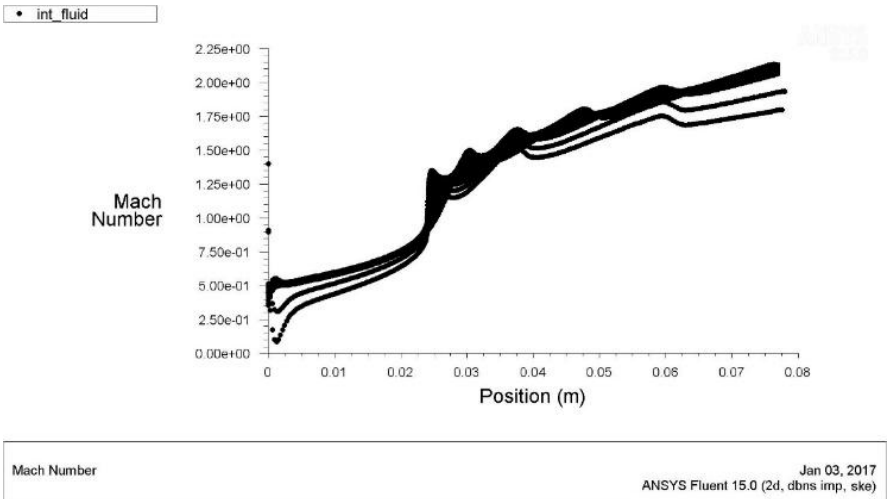

Figure 7: Mach Number Plot 4.76° Nozzle Angle

Mach number graph for 4.76° nozzle angle shows the formation of oblique shock waves after Mach number 1.7 because there is a little fall in Mach number [1], [5], [12]. This fall in Mach number occurs due to small backflow near the walls of the nozzle. In the same way, an oblique shock has appeared at the location

of0.04m, 0.05m, and 0.06m. Finally measured Mach number at the exit section is 2.13. The velocity at the outlet section is in between 509.36 m/sec to 536.17 m/sec.

Divergent Angle 7°

Static pressure at the entrance of the nozzle is found in between 2.26e+05 Pa to 2.60e+05 Pa. Pressure in the middle of the convergent section is around 2.26e+05 Pa and it is decreased up to 1.6e+05 Pa at the throat section. It is increased at the position of the third shock from -7.25e+04 Pa to -3.93e+04 Pa and also on the first position of shock. After traveling a little distance again the value of pressure got down to -7.26e+04 Pa at the exit section. As compared to the previous case pressure at the throat is a little bit decreased and at the outlet, it is decreased significantly.

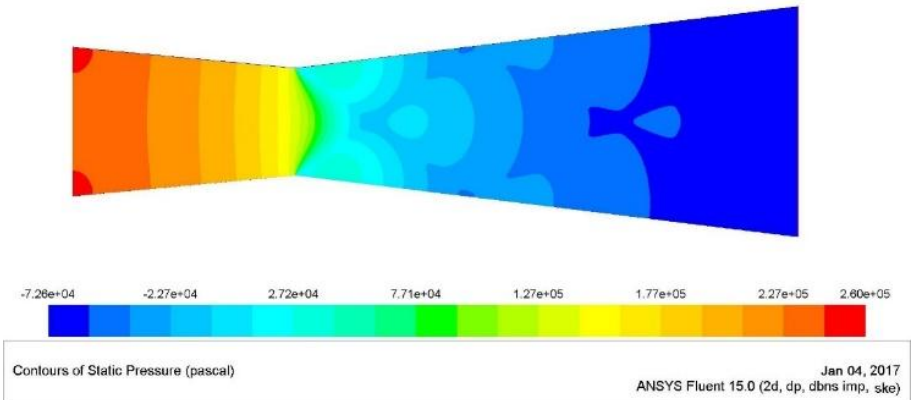

Figure 8: StaticPressure Contour at 7° Nozzle Angle

In the Mach number contour, it can be observed the variation in Mach number when the nozzle angle is changed to 7°. At the entrance of the nozzle, it is found in the range of 0.39 to 0.59. In the middle of the convergent section, it became around 0.68 and at the throat, it is in the range of 0.88 to 0.98. From the graph of the Mach number, it can be seen that in this case there are 4 shocks which are less as compare to the nozzle at 4.76°. At first shock Mach number got down to 1.47 from 1.57 and after this again increment in Mach number is found. After the complete expansion of fluid within the nozzle it is found between 2.27 to 2.37 at the exit section.

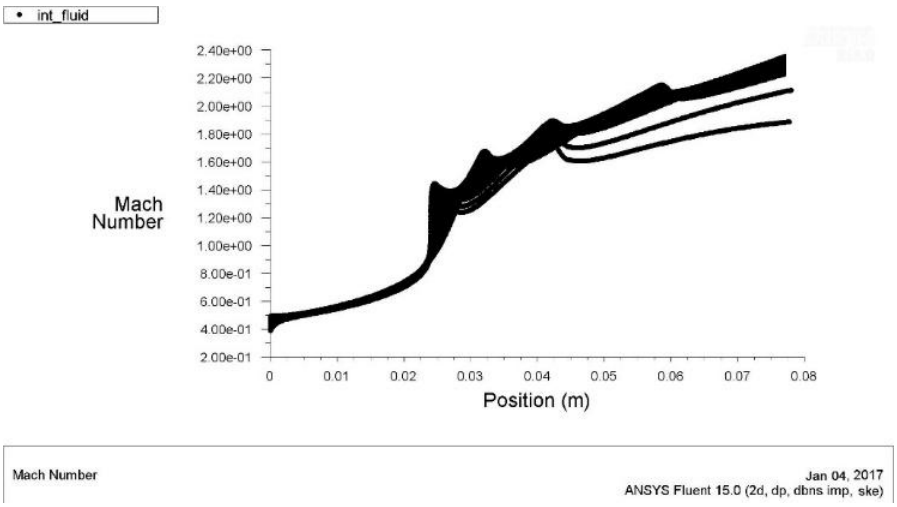

Figure 9: Mach Number Plot at 7° Nozzle Angle

As it is previously mentioned that the velocity graph will also show the approximately same pattern as of Mach number so from velocity contour we can see that velocity distribution is different in this case than that of the previous case. At the entry of the nozzle, the velocity is in between 141.24 m/sec to 169.49 m/sec. Velocity increased from 169.49 m/sec to 310.73 m/sec up to throat section corresponding to Mach number variation from 0.58 to 0.98. After the throat, there is a continuous increment in velocity due to the expansion of fluid but at the first shock, the decrease in velocity for a little distance is found. Velocity got down to 423.73 m/sec from 451.98 m/sec corresponding to Mach number from 1.57 to 1.47. At the exit section of the nozzle, velocity is found in between 536.73 m/sec to 564.98 m/sec. The increment can be observed in outlet velocity as compared to the previous case.

Divergent Angle 9°

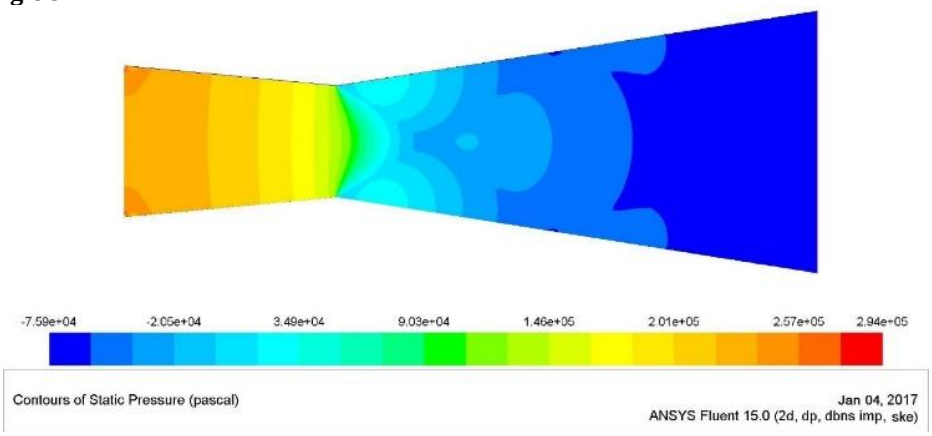

Figure 10: StaticPressure Contour at 9° Nozzle Angle

Static pressure at an inlet near the walls of the nozzle is around 2.56e+05 Pa. In the staring of flow near the inlet section, the pressure is found in the range of 2.19e+05 Pa to 2.38e+05 Pa. A drop is found at the throat of the nozzle and pressure reduced up to 1.45e+05 Pa which is less than that of the previous case. After this fluid is expanded in the divergent section and pressure is reduced continuously.There is a sudden increment in pressure at the first shock. Pressure increased at this shock is about -2.05e+04 Pa from -3.90e+04 Pa. -7.59e+04 Pa pressure is observed at the exit section. It is noticed that as the nozzle angle is increased outlet pressure is reduced which is good to achieve the objective of this paper.

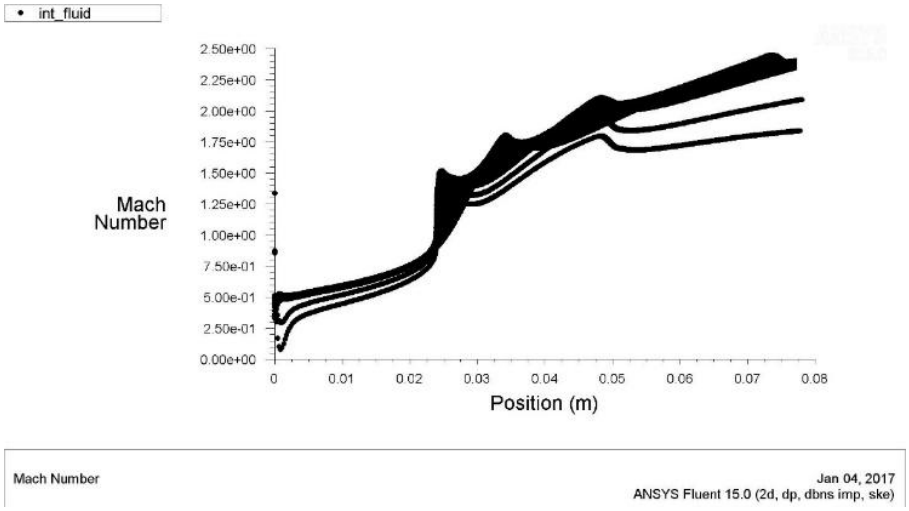

Figure 11: Mach Number Plot at 9° Nozzle Angle

Mach number at the inlet section is observed between 0.43 to 0.55. In the middle of the convergent section, it is around 0.67, and corresponding to it the velocity is 229.46 m/sec. At throat Mach number lies in the range of 0.79 to 0.99. Velocity at the throat is in between 286.82 m/sec to 315.51 m/sec. which is more than that of all previous cases. As the fluid moves further there is an increment again in Mach number is observed. The first little fall in Mach number is observed at first shock which is 1.38 from 1.49. Again two more shocks are observed from the Mach number graph for 9° divergent angle nozzle. Finally, in the exit section, a 2.45 Mach number is observed which is more than that of the previous case.

It is also observed here the number of shocks in the divergent section of the nozzle is reduced to 3 which is good to go. There is a decrement in velocity with regards to the first shock observed in the Mach number graph. This decreased velocity from 435.19 m/sec is 423.34 m/sec. For the next two shocks, a very small decrement in velocity is observed. At the exit section of the nozzle, velocity is in the range of 544.97 m/sec to 573.65 m/sec. Again some increment in outlet velocity is observed in this case.

Divergent Angle 9.5°

The below contour depicts the variation in static pressure when the nozzle angle is changed to 9.5°. Here the pressure at the inlet of the nozzle is between 2.32e+05 Pa to 2.50e+05 Pa. After that, as flow moves

towards the outlet section, a decrement in pressure is observed in the middle of the convergent section which is 2.32e+05 Pa. At the throat, the pressure is found in 1.46e+05 Pa to 1.63e+05 Pa range. It is known that after passing from the throat in the divergent section of the nozzle pressure will fall because of the expansion of fluid but a sudden increment is found at the first shock developed. The increased pressure is -2.76e+04 Pa from -4.49e+04 Pa. After this, a significant fall in pressure is found at the exit section which is between -6.23e+04 Pa to -7.97e+04 Pa. This significant decrease in outlet pressure as compared to the previous case of the 9° nozzle angle, is very helpful to achieve the objective.

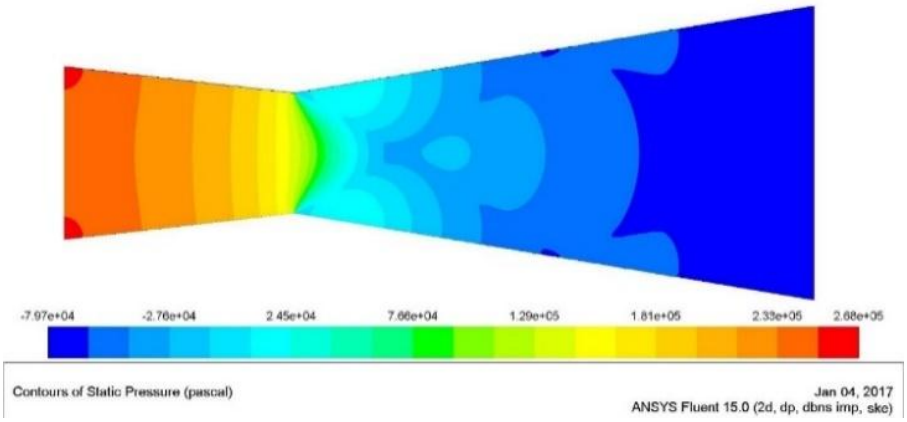

Figure 12: StaticPressure Contour at 9.5° Nozzle Angle

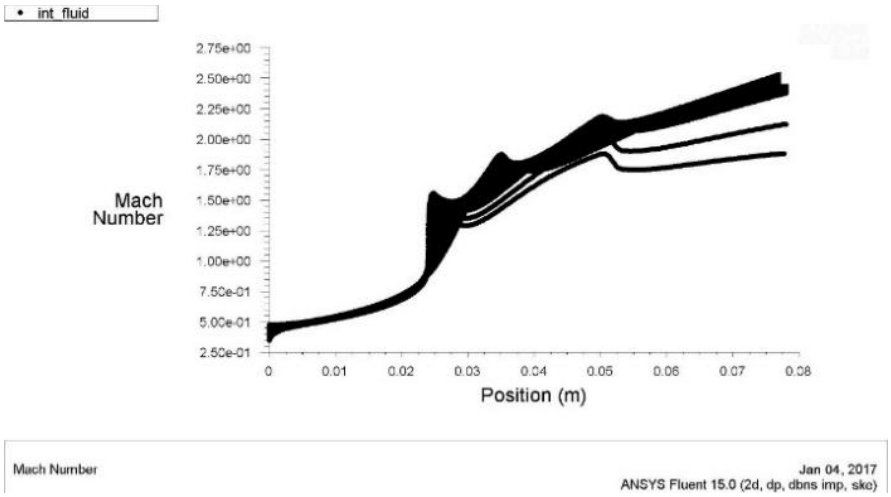

Figure 13: Mach Number Plot at 9.5° Nozzle Angle

Mach number at the inlet near the walls is found in the range of 0.35 to 0.46. At the entrance, region velocity is measured in between 146.01 m/sec to 175.22 m/sec. The entrance region is of subsonic flow where formation of a shock wave is always impossible [1]. As the fluid moves further Mach number in the middle of the convergent section is found between 0.57 to 0.68 and corresponding to this velocity is found in the range of 175.22 m/sec to 204.42 m/sec. At the throat section, Mach number lies in between 0.90 to 1.03, and velocity at the throat is in the range of 292.03 m/sec to 321.24 m/sec which is more than that of all previous cases. As the expansion of fluid started after passing from the throat first shock is observed at 0.023m and it is clear from the Mach number plot for this case. At this shock, there is a sudden decrement in Mach number as well as a sudden increment in the flow velocity. The incremented velocity is 496.46 m/sec from 467.25 m/sec and corresponding to this sudden velocity increment the Mach number variation is 1.67 from 1.78.

Finally, in the exit section, a 2.55 Mach number is observed which is the greatest at the outlet section among all the cases. For this Mach number corresponding, outlet velocity is found in between 554.87 m/sec to 584.07 m/sec which is the greatest value among all the cases and there is a 9 % increment in outlet velocity concerning the first case which is for 4.76° nozzle angle.

Divergent Angle 9.501°

Negative pressure is found in the entire domain of flow. Only a very high-pressure range 4.74e+10 Pa to 4.99e+10 Pa is observed in a particular vicinity of the divergent section. This is all because of high backflow in

the nozzle due to which complete flow in the divergent section became a reversible flow. Vector contour in fig-18 is shown for this case which depicts the clear picture of reverse flow inside the nozzle.

Divergent Angle 10°

Again a huge amount of backflow near the nozzle wall in the divergent section is found in this case.

Comparison of Results

The comparison graphs are presented in fig. 14 & 15. These are plotted with the help of numerical data obtained by taking the average of values at 20 cross-sections throughout the nozzle from inlet to outlet. Both of these graphs show that the maximum outlet velocity is achieved for a nozzle of the divergent angle of 9.5°.

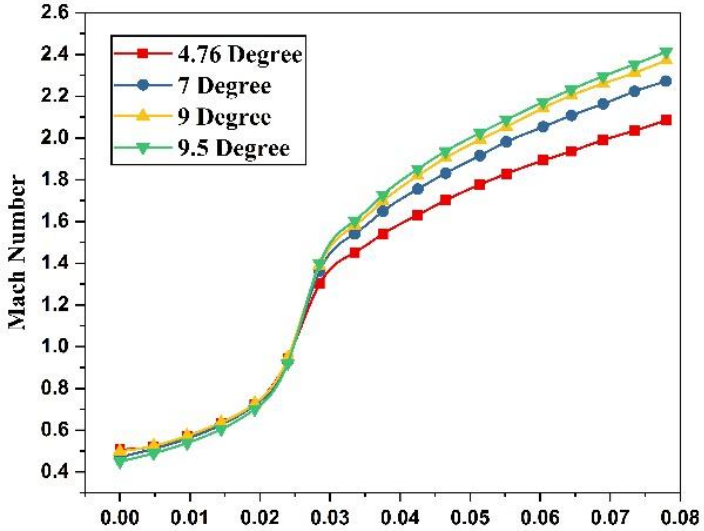

Figure 14: Graphical Comparison Of Mach Number For The Different Nozzle Angles

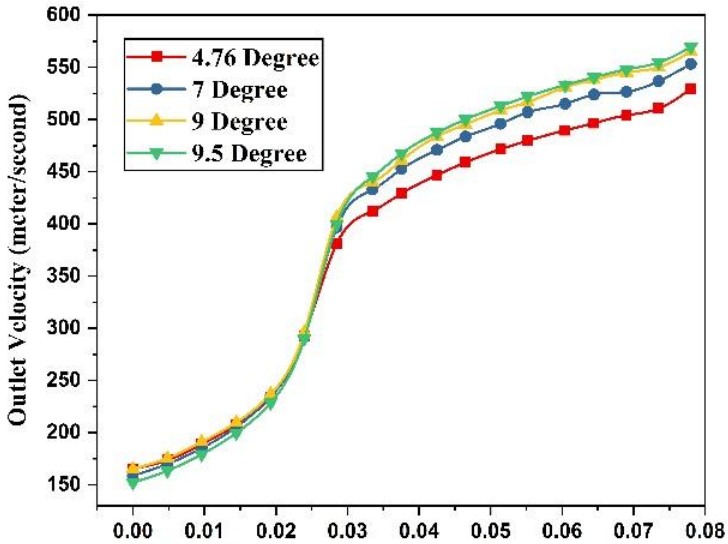

Figure 15: Graphical Comparison Of Outlet Velocity For The Different Nozzle Angles

Table6:Values of pressure, velocity and Mach Number for different nozzle angles

Nozzle Angle	Average Outlet Pressure (Pascal)	Average Outlet Velocity (m/sec)	Average Mach number at Exit Section
4.76°	-56632.81	529.39	2.08
7°	-68027.80	553.36	2.27
9°	-72866.95	564.95	2.37
9.5°	-74625.99	569.53	2.41
9.501°	Reverse Flow	Reverse Flow	Reverse Flow
10°	Reverse Flow	Reverse Flow	Reverse Flow

VII. LIMITATIONS OF THE STUDY

CD Nozzle analysis is carried out at certain inlet and outlet conditions. The study of the nozzle is done assuming the steady-state conditions of fluid flow. The flow is taken to be turbulent thus the study is not applicable for certain applications.

VIII. CONCLUSION

The design of the C-D nozzle was carried out based on the optimization of the nozzle divergent angle for the maximization of corresponding outlet velocity. It is found after the study that the 9.5o nozzle angle is the best suited for the maximum outlet thrust and velocity. A further small variation of 0.01o in the nozzle angle leads to reverse flow in the divergent section which is not acceptable because high negative pressure is observed in the whole flow region.

The nozzle of 18 mm wide inlet, 12.5 mm wide throat and 30.58 mm wide outlet is found as the best nozzle for the maximum outlet velocity and thrust considering the particular operating parameters.

NOMENCLATURE

T – Temperature of fluid (Kelvin, K)

p – Pressure of fluid (Newton/meter^2, N/m^2)

ρ – Density of fluid (kilogram/meter^3, kg/m^3)

A – Cross-sectional area (meter^2, m^2)

M – Mach number

C – Velocity of sound (meter/second, m/sec)

$_1$ – Subscript used for inlet values

$_2$ – Subscript used for outlet values

$_*$ – Superscript used for throat values

ṁ – Mass flow rate (kilogram/second, kg/sec)

Υ – Adiabatic index

V – Local flow velocity (meter/second, m/sec)

v – Specific Velocity of flow

v' – Specific volume of the fluid

V' – Volume of the fluid (meter^3, m^3)

R – Gas Constant

μ_t – Eddy Viscosity (Newton-second/meter^2, Ns/m^2)

κ – Turbulent Kinetic Energy (meter^2/second^2, m^2/sec^2)

ε – Turbulent Dissipation Rate (meter^2/second^3, m^2/sec^3)

G – Turbulent Generation Rate

σ_κ – Constant

σ_ε – Constant

$C_{1\varepsilon}$ – Constant

$C_{2\varepsilon}$ –Constant

ACKNOWLEDGMENT

We would like to thank and express profound regards to Mr. Kuldeep Dagar, the senior researcher University of Nottingham, UK. Mr. Dagar spent countless hours directing us towards the successful completion of this work. Assistant professor Sanjeev Kumar Gupta, Mechanical Engineering department, GLA University, Mathura is also greatly acknowledged for arranging the CFD lab facility to complete this work.

REFERENCE

[1]. S. M. Yahya, "Fundamentals of Compressible Flow with Air Craft And Rocket Propulsion", New Age International (P) Limited, Publishers, Fifth Edition, 2016.

[2]. H. Qiu, C. Xiong, W. Fan, "One-dimensional unsteady design method for pulsed detonation engine nozzles", Journal of Aerospace Engineering, vol. 228, issue 13, pp. 2496–2507, 2014.

[3]. Q. Zhang, W. Fan, K. Wang, W. Lu, Y. Chi, Y. Wang, "Impact of nozzles on a valveless pulse detonation rocket engine without the purge process", Applied Thermal Engineering, vol. 100, pp. 1161-1168, 2016.

[4]. K. P. S. Surya Narayana, K. S. Reddy, "Simulation of Convergent Divergent Rocket Nozzle using CFD Analysis", IOSR Journal of Mechanical and Civil Engineering, vol. 13, issue 4, ver. I, pp. 58-65, 2016.

[5]. D. D. Majil, "Optimization of Nozzle Parameters for Various Thrust Vectoring Nozzle Using CFD", Discovery, The International Journal, pp. 2370-2378, 2016.

[6]. K. M. Pandey, A. P. Singh, "CFD Analysis of Conical Nozzle for Mach 3 at Various Angles of Divergence with Fluent Software", International Journal of Chemical Engineering and Applications, vol. 1, no. 2, pp. 179-185, 2010.

[7]. B. Kuttan P., M. Sajesh, "Optimization of Divergent Angle of a Rocket Engine Nozzle Using Computational Fluid Dynamics", The International Journal Of Engineering And Science, vol. 2, issue 2, pp. 196-207, 2013.

[8]. G. Satyanarayana, Ch. Varun, S. S. Naidu, "CFD Analysis of Convergent-Divergent Nozzle", ACTA Technical Corviniensis-Bulletin of Engineering, vol. VI, issue 3, pp. 139-144, 2013.

[9]. G. R. Rao, U. S. Ramakanth, A. Lakshman, "Flow Analysis in a Convergent-Divergent Nozzle Using CFD", International Journal of Research in Mechanical Engineering, vol. 1, issue 2, pp. 136-144, 2013.

[10]. K. G. Vishnu, A. K. Mubarak, "Analysis of Flow Structure by Varying Divergence Angle and Contour of Supersonic C-D Nozzles", International Journal of Engineering Research in Mechanical and Civil Engineering, vol. 2, issue 7, pp. 28-34, 2017.

[11]. J.Wu, T. H. New, "An investigation on supersonic bevelled nozzle jets", Aerospace Science and Technology, vol. 63, pp.278-293, 2017.

[12]. S. Keir, R. Ives, F. A. Hamad, "CFD Analysis of C-D Nozzle compared with Theoretical & Experimental Data", Aerospace Europe 6th Council of European Aerospace Societies Conference, paper no. 943, pp. 1-11, 2017.

Goyal S, et. al. "CFD Analysis of Supersonic C-D Nozzle for Optimization of Divergent Angle." *The International Journal of Engineering and Science (IJES)*, 10(03), (2021): pp. 33-43.